Palaeogeography, Palaeoclimatology, Palaeoecology xxx (xxxx) xxx–xxx

Contents lists available at ScienceDirect

Palaeogeography, Palaeoclimatology, Palaeoecology

journal homepage: www.elsevier.com/locate/palaeo

Neuroanatomy of the ankylosaurid dinosaurs *Tarchia teresae* and *Talarurus plicatospineus* from the Upper Cretaceous of Mongolia, with comments on endocranial variability among ankylosaurs

Ariana Paulina-Carabajal[a,*], Yuong-Nam Lee[b], Yoshitsugu Kobayashi[c], Hang-Jae Lee[d], Philip J. Currie[e]

[a] Instituto de Investigaciones en Biodiversidad y Medioambiente, CONICET - Universidad Nacional del Comahue, San Carlos de Bariloche 8400, Argentina
[b] School of Earth and Environmental Sciences, Seoul National University, Seoul 08826, South Korea
[c] Hokkaido University Museum, Hokkaido University, Sapporo 060-0810, Japan
[d] Geological Museum, Korea Institute of Geoscience and Mineral Resources, Daejeon 34132, South Korea
[e] Department of Biological Sciences, University of Alberta, Edmonton T6G 2E9, Canada

ARTICLE INFO

Keywords:
Braincase
Cranial endocast
Paleoneurology
Ankylosauridae

ABSTRACT

Ankylosaur braincase and endocranial morphologies are poorly known. Furthermore, cranial endocasts have been described for fewer than ten taxa so far. The complete inner ear morphology is known for only three species – *Euoplocephalus tutus*, *Kunbarrasaurus ieversi*, and *Pawpawsaurus campbelli*. Here, the first cranial endocast morphologies are presented for the Mongolian Cretaceous ankylosaurids *Talarurus plicatospineus* and *Tarchia teresae*. The study of paleoneurological features of these Mongolian taxa adds novel anatomical information to both species allowing the first comparison with ankylosaurids from North America. The development of a cerebellar flocculus that leaves an impression on the vestibular eminence – floccular recess – is observed in *Euoplocephalus*, *Talarurus* and *T. teresae*. Because this structure hasn't been identified in any nodosaurid so far, its presence in ankylosaurid cranial endocasts may represent a possible synapomorphy with unknown paleobiological implications.

1. Introduction

Braincase morphology is poorly known for some groups as is the case for ankylosaurs, a clade of quadruped herbivorous ornithischians known from the Middle Jurassic to the Upper Cretaceous (e.g., Galton, 1983; Vickaryous et al., 2004; Thompson et al., 2012). Ankylosaurs have highly ossified skulls with cranial ornamentation that obliterates most sutures (Vickaryous et al., 2004; Thompson et al., 2012). Because of this, in complete ankylosaur skulls the lateral and ventral sides of the braincase are often obscured by other skull bones, if not by sediment, and it is unusual to find a skull that shows the internal morphology without the aid of X-ray computed tomography (CT). Moreover, even with CT scans, many ankylosaur skulls do not yield detailed, clean endocranial data due the size, robustness and morphology of their skulls. Detailed braincase descriptions have been made of several species including the nodosaurid *Pawpawsaurus campbelli* (Lee, 1996; Paulina-Carabajal et al., 2016a) and the ankylosaurids *Euoplocephalus* (Vickaryous and Russell, 2003), *Bissektipelta* (="*Amtosaurus*", Averianov, 2002; Parish and Barrett, 2004; Arbour and Currie, 2016), and *Talarurus plicatospineus* (Tumanova, 1987). Endocranial descriptions have been done based on fragmentary braincases – *Pinacosaurus granger* (Tumanova, 1987, her fig. 8), *Saichania chulsanensis* (Maryańska, 1977), *Talarurus plicatospineus* (Tumanova, 1987, her fig. 7) – whereas several cranial endocasts were studied using artificial cranial endocasts. These digital or latex cranial endocasts are known for nine species, including the basal ankylosaur *Kunbarrasaurus ieversi* (Leahey et al., 2015), the ankylosaurid *Euoplocephalus tutus* (Coombs, 1978; Witmer and Ridgely, 2008; Miyashita et al., 2011), and the nodosaurids *Cedarpelta bilbeyhallorum* (Carpenter et al., 2001), *Hungarosaurus tormai* (Ősi et al., 2014), *Panoplosaurus mirus* (Witmer and Ridgely, 2008), *Pawpawsaurus campbelli* (Paulina-Carabajal et al., 2016a), cf. *Polacanthus* sp. (Norman and Faiers, 1996), *Struthiosaurus austriacus* and *S. transylvanicus* (Pereda Suberbiola and Galton, 1994), and an unnamed nodosaurid from Japan (Hawakaya et al., 2005).

Mongolian ankylosaurs include several species with known skulls such as *Pinacosaurus grangeri* (Gilmore, 1933; = *P. ninghsiensis* Young, 1935), *Minotaurasaurus ramachandrani* (Penkalski and Tumanova, 2017, contra Arbour et al., 2014), *Saichania chulsanensis* (Maryańska,

* Corresponding author.
E-mail address: a.paulinacarabajal@conicet.gov.ar (A. Paulina-Carabajal).

https://doi.org/10.1016/j.palaeo.2017.11.030
Received 20 June 2017; Received in revised form 11 November 2017; Accepted 11 November 2017
0031-0182/ © 2017 Published by Elsevier B.V.

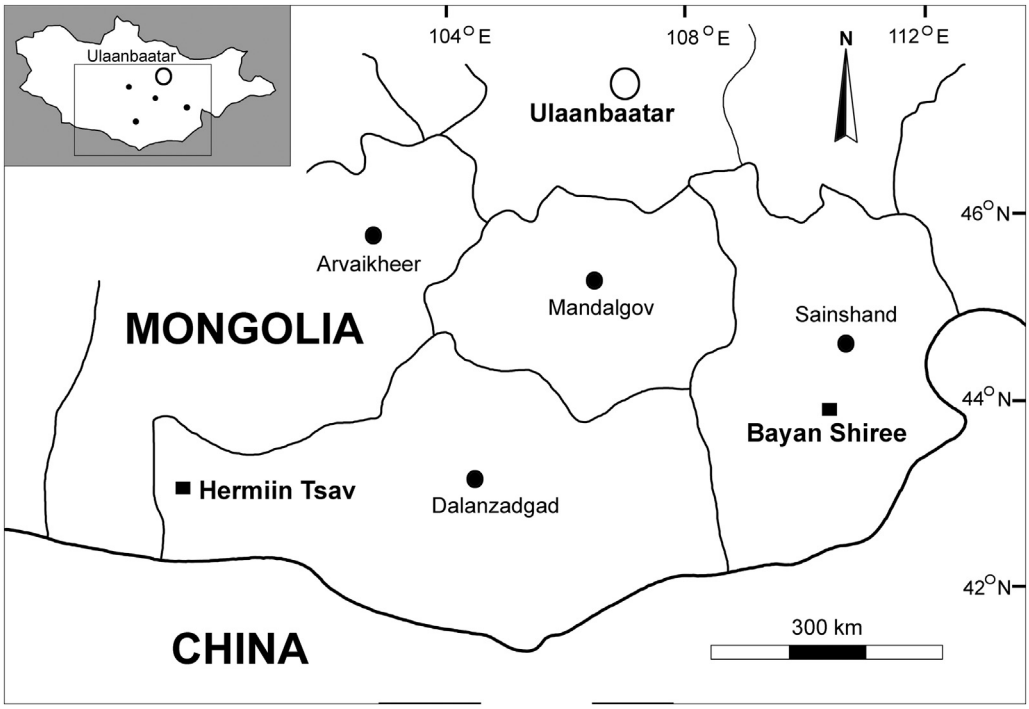

Fig. 1. Location map indicating the provenance localities of the skulls of *Talarurus* (MPC-D 100/1354) and *Tarchia teresae* (MPC-D 100/1353).

1977), *Talarurus plicatospineus* (Maleev, 1952), *Tarchia kielanae* (Maryańska, 1977), *Zaraapelta nomadis* (Arbour et al., 2014) and *Tarchia teresae* (Penkalski and Tumanova, 2017). However, in the particular case of ankylosaurids, the neuroanatomy is better known for *Euoplocephalus* from North America (Witmer et al., 2008; Miyashita et al., 2011). In this paper, the braincase morphology and paleoneurology of the Mongolian taxa *Talarurus plicatospineus* and *Tarchia teresae* is described and analyzed using CT scans. The study of paleoneurological features of these Mongolian taxa adds novel anatomical information to both species allowing the first comparison with ankylosaurids and nodosaurids from North America.

2. Materials and methods

The specimens in the present study were recovered by the Korea-Mongolia International Dinosaur Expedition (2007–2008), and were prepared at the Hwaseong City laboratory and the Korea Institute of Geoscience and Mineral Resources (KIGAM). The skull of *Talarurus plicatospineus* (MPC-D 100/1354) was excavated from the Bayanshiree Formation (Cenomanian-Santonian), Bayanshiree locality of the eastern Gobi (GPS: 44° 16′31.56″ N, 109° 54′3.78″ E) (Fig. 1). Although most of the right side of the skull is missing by breakage, the braincase region is practically complete, although it shows some degree of diagenetic deformation that causes the endocranial structures not to be symmetrically located in the digital reconstruction (Fig. 2). The skull of *Tarchia teresae* (MPC-D 100/1353; Fig. 2) was excavated from Hermiin Tsav locality from the southern Gobi (GPS: 43° 28′4.32″ N, 99° 53′28.86″ E) (Fig. 1). It was found, associated with a partial fibula of *Tarbosaurus*, in a yellow greyish-brown sandstone layer of Lower Maastrichtian age corresponding to the Nemegt Formation (Eberth, in press). The complete skull shows diagnostic features of *Tarchia teresae* such as unfused quadrate and paroccipital process, and bifurcated opening for CNs IX–XII (Penkalski and Tumanova, 2017). The braincase is undistorted except for large anteroposterior fractures on the left and right sides, which displaced the basicranium few millimeters from the lateral walls (Fig. 3). The taxonomy followed in this paper for the identification of the skull of *Tarchia* is that of Penkalski and Tumanova (2017).

Both specimens were CT scanned using an industrial X-ray tomographer made in the KIGAM facilities. A set of 402 slices was made for *Talarurus* and two sets of slices (one including the complete length of the skull and another focused on the braincase region) were made for *T. teresae* (728 and 339 slices respectively). The slices were taken at 0.5 mm intervals, using a voltage of 215.0 kV and current of 300 μA; the Field of View is of 56.05 cm. The thicknesses of the skull bones obscured small neurovascular passages and most of the semicircular canals of the inner ear. The CT scans of *T. teresae* have some "noise" on the dorsal surface of the skull roof. This was produced by the sum of millimetric vertical oscillation movements during the rotation of the skull over its main axis during CT scanning, and does not affect the observation of the endocranial cavity.

For comparison purposes, CT images of the North American nodosaurid *Panoplosaurus* (= *Edmontonia*, ROM 1215) were downloaded from the Witmerlab webpage at http://www.ohio.edu/people/witmerl/DinoSinuses_main.htm#CT%20scan%20data.

Segmentations were made using the software Materialise Mimics 18.0 (Materialise Inc., Leuven, Belgium), and final illustrations for publication were made using Adobe Photoshop (CS3).

Institutional abbreviations: FWMSH, Fort Worth Museum of Science and History, Fort Worth; KIGAM, Korea Institute of Geoscience and Mineral Resources; MPC, Institute of Paleontology and Geology, Mongolian Academy of Sciences, Ulaanbaatar, Mongolia; ROM, Royal Ontario Museum, Toronto, Canada; USNM, National Museum of Natural History, Smithsonian Institution, Washington, USA; YPM, Yale Peabody Museum, New Haven, USA; ZPAL, Palaeozoological Institute, Polish Academy of Sciences, Warsaw.

3. Results

3.1. Neuroanatomy of Talarurus plicatospineus

3.1.1. General braincase morphology and neurovascular foramina

The braincase of *Talarurus* was digitally isolated from the other skull bones to observe the lateral walls and cranial foramina (Fig. 4). The occipital condyle is kidney-shaped in posterior view and projects posteroventrally. The neck of the occipital condyle is short and the ventral margin is smooth, unlike the keeled margin in *T. tresae*. Lateral to the

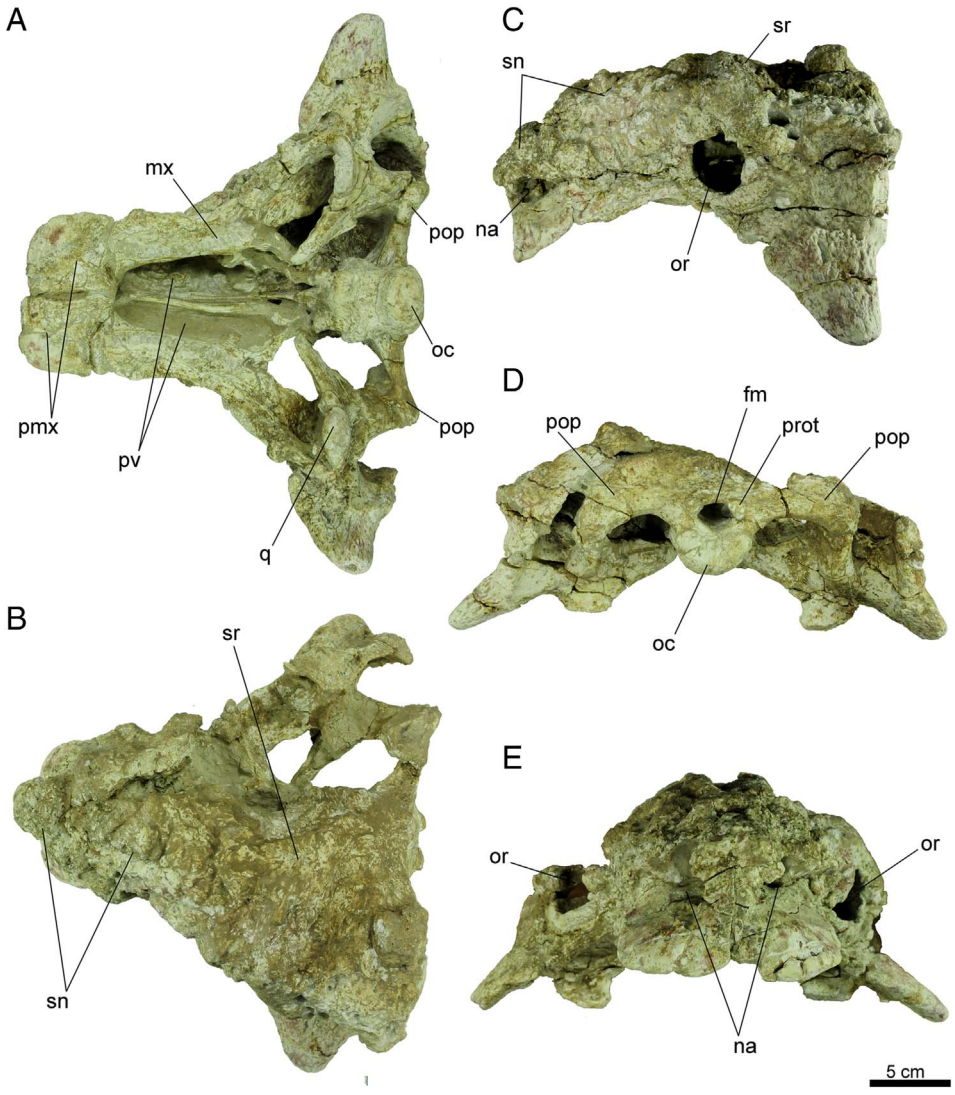

Fig. 2. Photographs of the skull of *Talarurus* (MPC-D 100/1354) in ventral (A), dorsal (B), lateral (C), posterior (D) and anterior (E) views. Abbreviations: fm, foramen magnum; mx, maxilla, na, narina; oc, occipital condyle; or, orbit; pmx, premaxilla; prot, protuberance; pv; q, quadrate; sn, snout; sr, skull roof. Scale bar = 5 cm.

occipital condyle there are two foramina. The most posterior foramen is oval and is subdivided internally into two foramina for branches of cranial nerve (CN) XII, which merge distally before exiting the braincase (Figs. 4B, 5). The larger middle foramen corresponds to a recess in which open the metotic foramen (for CNs IX–XI) anteriorly, and a foramen for a separate anterior branch of CN XII posteriorly (Fig. 4B). The most anterior foramen is a probable small fenestra ovalis, at the base of the paroccipital process and anteroventral to the metotic foramen (Fig. 4B). The internal extent of the columellar recess is not observed in the CT scan (neither the inner ear), which makes it impossible to identify the later as the fenestra ovalis. Kurzanov and Tumanova (1978) suggested that the fenestra ovalis and the metotic foramen are separated ventrally by an incomplete crista interfenestralis in *Talarurus*, but this trait is not observed in the specimen under study.

The basisphenoid forms most of the basicranium, which is low but robust. Endocranially, there is no medullar eminence and the dorsum sellae is low and projects slightly dorsally. The foramen for the cerebral branch of the internal carotid artery is large and slit-like, and opens onto the lateral side of the basisphenoid (Fig. 4B). The ventral portion of the internal carotid foramen is continuous with a groove that extends anteroventrally initially but then converges ventromedially with its counterpart between both basipterygoid processes (Fig. 4). These grooves are probably left by the median common carotid artery and the paired internal carotid arteries, as described for crocodiles (Porter et al., 2016). The foramen for CN VI is small and opens anterodorsal to the internal carotid artery foramen.

The laterosphenoid forms a small protuberance where it contacts the epipterygoid (which is fused to the lateral wall of the braincase, but was removed digitally in Fig. 4) close to the laterosphenoid-frontal contact. The postorbital process of the laterosphenoid is a transverse ridge of bone that distally becomes a dorsoventrally compressed expansion attached to the ventral side of the frontal. Cranial nerves V and VII exit the braincase separately but through foramina inside a single recess, which is irregular in shape (Fig. 4B). The foramen for CN VII is smaller, and pierces the prootic, whereas the anterior margin of the recess is probably formed by the laterosphenoid as in most dinosaurs (Currie, 1997). All the branches of CN V leave the endocranial cavity though the same passage. The orbitocerebral vein pierces the laterosphenoid dorsal to CN V near to the contact with the frontal bone (Fig. 4B). This suggests that the laterosphenoid extends slightly anterior and dorsal to the orbitosphenoids, which are in turn displaced anteroventrally, where they contact each other at the midline.

The foramen for CN II is large and is positioned anterior to CN V, probably enclosed by the orbitosphenoid. Each foramen is separate from its counterpart by ossified interorbital septum and ethmoidal elements. Separate cranial foramina for nerves III and IV can neither be observed in the braincase nor in the CT scans, suggesting that those nerves exit the endocranial cavity together with CN II. In front of the orbitosphenoids, the olfactory tracts and bulbs are enclosed by ossified ethmoidal elements. Sutures are not visible and neither is the foramen

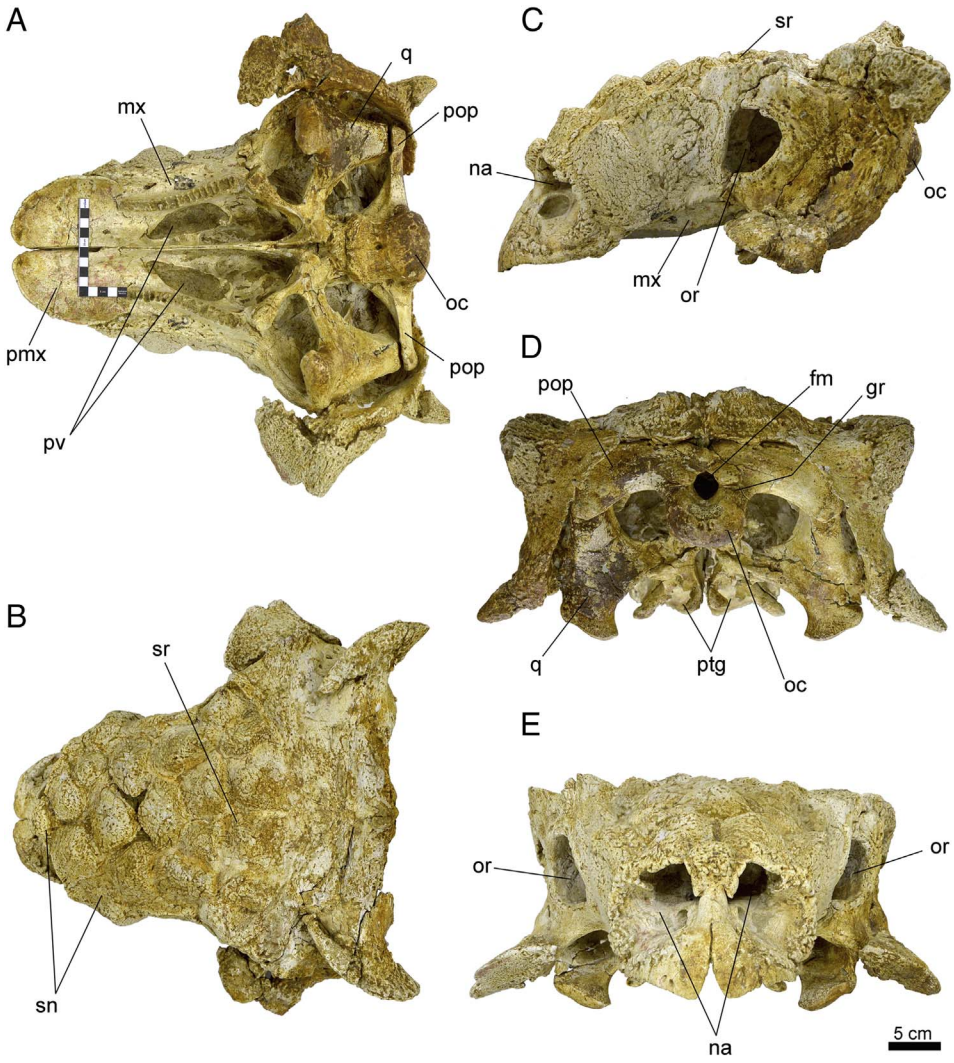

Fig. 3. Photographs of the skull of *Tarchia teresae* (MPC-D 100/1353) in ventral (A), dorsal (B), lateral (C), posterior (D) and anterior (E) views. Abbreviations: idem Fig. 1. Scale bar = 5 cm.

for CN I, which opens anteriorly within the nasal cavity.

3.1.2. Cranial endocast

The general morphology of the endocast of *T. plicatospineus* is reminiscent of those of *Euoplocephalus* (Miyashita et al., 2011) and *T. teresae*, with the forebrain, midbrain, and hindbrain forming a sigmoidal shape in lateral view (with poorly marked angles), laterally expanded cerebral hemispheres (Fig. 5), and large pituitary. The dorsal longitudinal sinus forms a small pointy dorsal expansion (= dural peak).

The outstanding features of the forebrain include the olfactory tract (olfactory bulbs are not reconstructed because they did not leave an

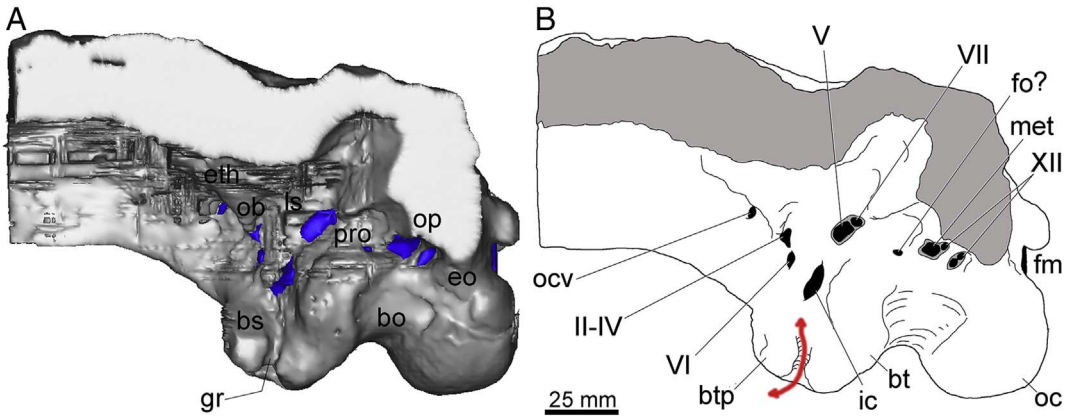

Fig. 4. Digital reconstruction (left) and line drawing (right) of the braincase of *Talarurus* (MPC-D 100/1354) in left lateral view. Abbreviations: bo, basioccipital; bs, basisphenoid; bt, basal tuber; btp, basipterygoid process; eo, exoccipital; eth, ethmoidal elements; ic, cerebral branch of the internal carotid artery; fo, fenestra ovalis; gr, groove for internal carotid artery; ls, laterosphenoid; met, metotic foramen (for CNs IX–XI and internal jugular vein); ocv, orbitocerebral vein; op, opisthotic; pro, prootic; II-XII, cranial nerves. The arrow indicates the groove for ic. Scale bar = 25 mm.

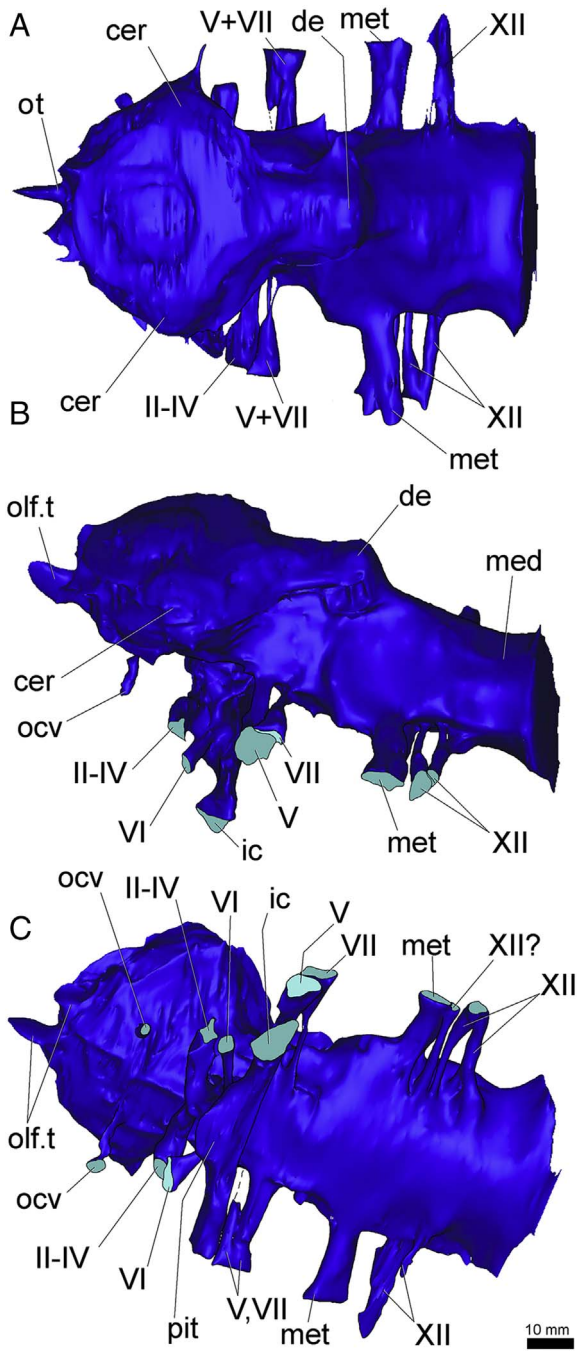

Fig. 5. Digital reconstruction of the cranial endocast of *Talarurus* (MPC-D 100/1354) in dorsal (A), left lateral (B) and lateroventral (C) views. Abbreviations: cer, cerebral hemisphere; de, dorsal expansion; ic, internal carotid artery; med, medulla oblongata; met, metotic passage (for CNs IX–XI); ocv, orbitocerebral vein; ot, olfactory tract; pit, pituitary; II-XII, cranial nerves. Scale bar = 10 mm.

impression on the ventral side of the frontals), the cerebral hemispheres, optic nerves (CN II), and the pituitary body. The cerebral hemispheres are not particularly large but are well differentiated laterally. The widest part of the endocast corresponds to the transverse section across the cerebral hemispheres. However, it is not markedly wider than the medullar region of the endocast, indicating that the cerebral hemispheres are not large when compared to other ornithischians such as hadrosaurids (e.g., Evans et al., 2009). The midline separation between the cerebral hemispheres is not visible indicating that the dura mater was thick and/or that there was a well-developed dorsal longitudinal sagittal sinus (Evans, 2006; Witmer et al., 2008).

The olfactory tract projects anteriorly in front of the cerebral hemispheres close to the midline; the olfactory bulbs are not visible. Cranial nerve II has large passages (probably used by CNs III and IV as well) that extend slightly anterolaterally from the ventral side of the endocast. The passages diverge anteriorly from the midline near to the infundibular stalk (Fig. 5B,C). The pituitary body is elongate and descends from the ventral surface of the endocast. Although the infundibular stalk projects ventrally, the pituitary body is inclined slightly posteroventrally. The distal end of the pituitary is continuous to the laterally projected passages for the cerebral branch of the internal carotid artery (Fig. 5C). There are no visible mesencephalic (midbrain) structures in the endocast (e.g. optic lobes and cranial nerves III and IV). As mentioned, a single large passage near the infundibular stalk region may represent the exit for cranial nerves II–IV.

The visible features of the hindbrain in the cranial endocast include the cerebellum, medulla oblongata and cranial nerves V–XII. In *T. plicatospineus*, the medulla oblongata is anteroposteriorly long and its ventral surface is smooth (Fig. 5B,C). The floccular process of the cerebellum is poorly observed in the CT scans of this specimen. However, the recess in the endocranial cavity that hosted the flocculus (the floccular recess) was described in the braincase of another specimen –although not recognized as this structure by Tumanova (1987, her fig. 7D), who said that "there is a dorsoposterior inclined depression on the endocranial wall that terminates blindly that may have had no connection with the membraneous labyrinth". Clearly, this "blind depression" on the anterior surface of the vestibular eminence corresponds to the floccular recess. The root of CN V is large and extends laterally (Fig. 5B). The passage for CN VII has a smaller diameter and extends parallel and slightly posterodorsal to the passage for CN V, to exit dorsally within the same recess (Fig. 5B, C). The root of CN VI is positioned anteroventral to CN V and lateral to the infundibulum (Fig. 5B). Its passage has a sigmoidal curvature, extending anteroventrally first and then anterolaterally to exit through a small foramen located ventral to CN II in the anterior section of the braincase (Fig. 4B). The metotic passage (for CNs IX–XI and internal jugular vein) is large and confluent distally with the anterior branch of CN XII, as in *Euoplocephalus* (Miyashita et al., 2011) (Fig. 5C). The CT scans of *T. plicatospineus* show that the two posterior branches of CN XII leave the endocranial cavity through two passages that merge distally to exit – separately – lateral to the occipital condyle within a single recess (Fig. 4B).

3.2. Neuroanatomy of Tarchia teresae

3.2.1. Braincase and neurovascular foramina

The braincase of *T. teresae* was digitally isolated from the other skull bones to allow the observation of the lateral side and its cranial foramina (Fig. 6). The elements forming the lateral wall of the braincase – orbitosphenoid, laterosphenoid, prootic and opisthotic – are fused and no clear sutures are observed, as in other ankylosaurs. Although the basicranium is anteroposteriorly longer than high, the braincase in general is anteroposteriorly short and low (as long as tall), and the basicranium represents 45% of the total height (Fig. 6B). The exoccipital forms the lateral margins of the foramen magnum and the dorsolateral portions of the occipital condyle. The foramen magnum is oval and taller than wide (Fig. 3D). Dorsolateral to the foramen magnum, the exoccipital protuberances are large, oval and strongly defined, unlike the poorly developed protuberances in *Saichania*. Each of the protuberances overhangs two horizontal grooves (4 mm in diameter) that extend laterally from the foramen magnum and become diffuse at the base of the paroccipital process (Fig. 3D). There is only one groove below the protuberance in *Saichania*, and the grooves are absent in *T. plicatospineus* (Fig. 2D). Kurzanov and Tumanova (1978) described these grooves as the first pair of spinal nerves; however, they more likely correspond to impressions left by vascular extensions of the dorsal longitudinal venous sinus (e.g., the "caudal head vein" in Porter

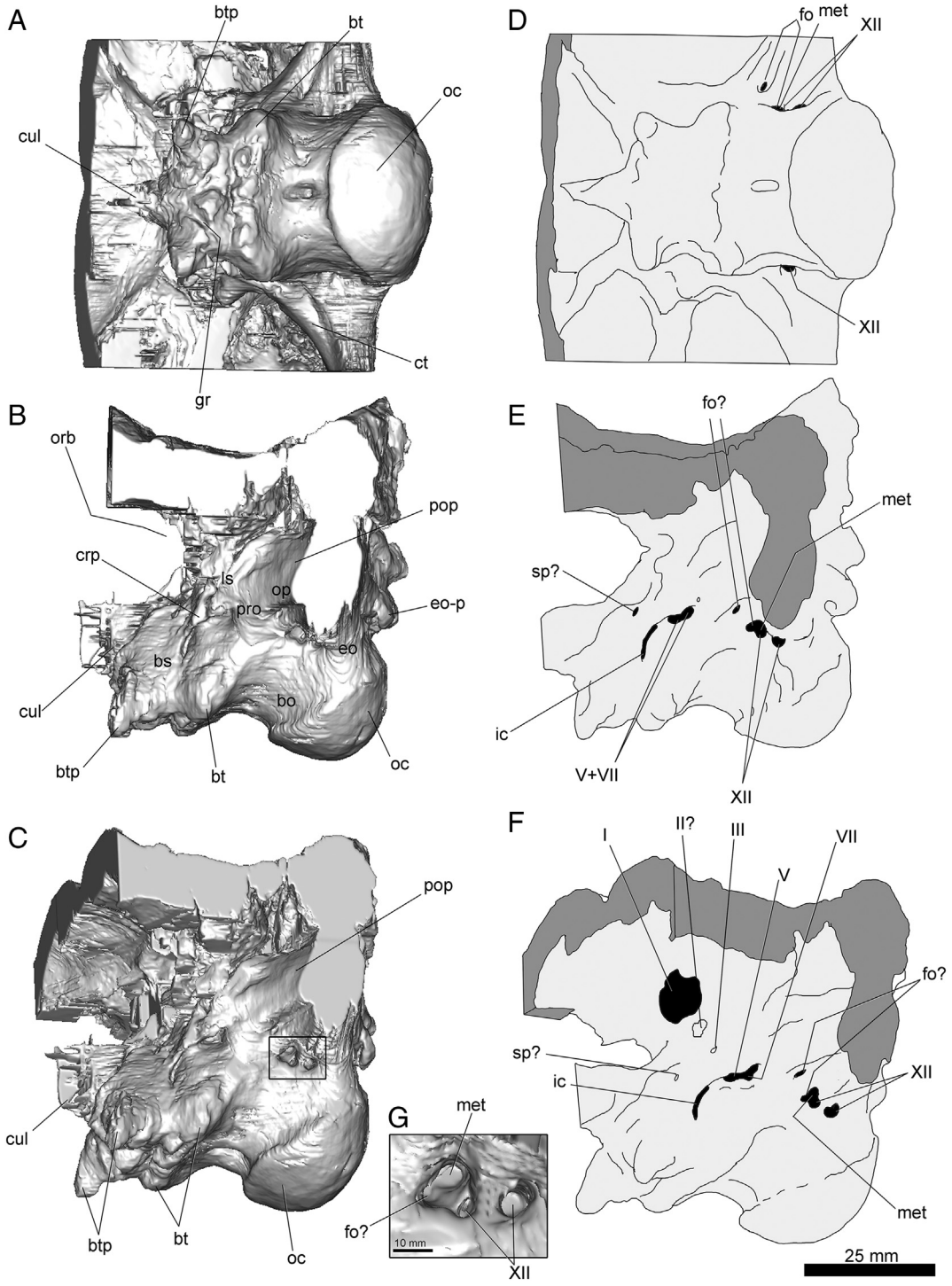

Fig. 6. Digital reconstruction (A–C,G) and line drawings (D–F) of the braincase of *Tarchia teresae* (MPC-D 100/1353) in ventral (A,D), left lateral (B,E) and lateroventral (C,F) views. Detail of posterior cranial foramina (D) showing the subdivisions within the larger foramen for CN XII (posteroventral), CNs IX–XI (dorsal) and possible fenestra ovalis (anterior). Abbreviations: bt, basal tuber; btp, basipterygoid process; crp, crista prootica; ct, crista tuberalis; cul, cultriform process; eo-p, exoccipital protuberance; fo, fenestra ovalis; gr, groove; ic, cerebral branch of internal carotid artery; met, metotic foramen (for CNs IX–XI); oc, occipital condyle; orb, orbit; sp., sphenoid artery; I–XII, cranial nerves. Scale = 25 mm and 10 mm in G.

et al., 2016). In *T. teresae*, the occipital condyle is hemispherical in posterior view, and inclined slightly posteroventrally. The ventral border of the condyle is keeled and bears an oval blind pit (Fig. 6A,D).

Lateral to the occipital condyle, there are two large cranial foramina (Fig. 6E,G). The most posterior foramen is subcircular and is completely enclosed by the exoccipital, corresponding to the exit of the posterior branches of CN XII. The anterior larger and irregular in shape foramen is a three-lobed opening that corresponds to the external opening for at least two –maybe three– passages that merge distally before exiting the braincase (Fig. 6G). Within this recess the posteroventral foramen corresponds to an anterior branch of CN XII, whereas the dorsal and larger foramen corresponds to the metotic foramen (CNs IX–XI) (Fig. 6G). A possible anterior foramen may represent a separate passage (it is not observed in the CT scans) for the columella or a neurovascular element (a separate CN IX or a blood vessel). Tumanova (1987) suggested that the metotic foramen converged with the fenestra ovalis in *T.*

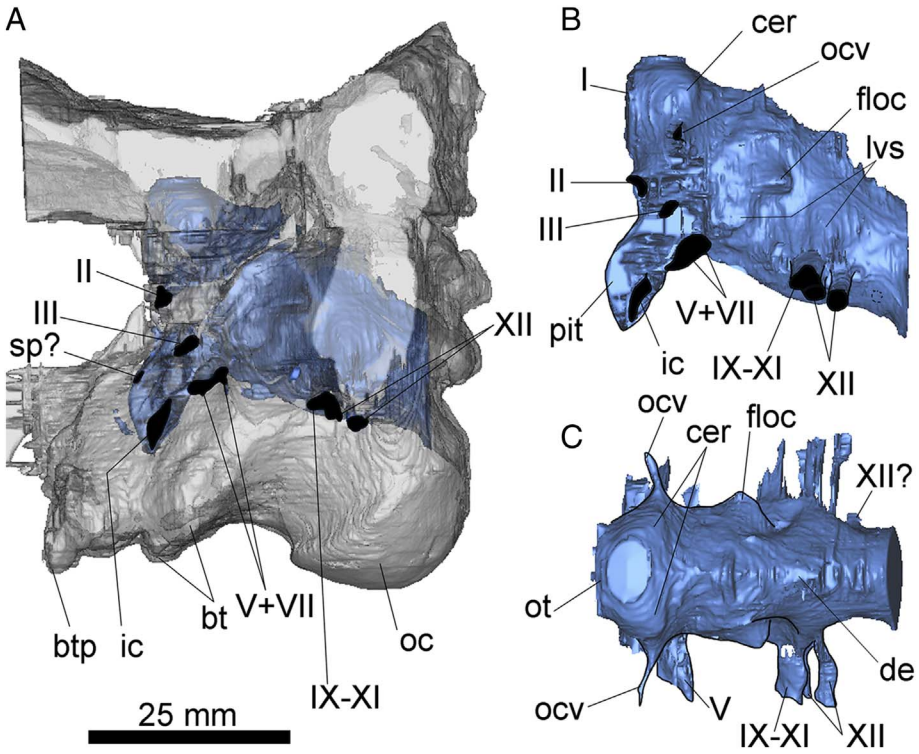

Fig. 7. Digital reconstruction of the braincase cranial endocast of *Tarchia teresae* (MPC-D 100/1353) in lateral (A,B) and dorsal (C) views. In the left figure, the bone is rendered semitransparent to allow observation of the endocranial cavity. Abbreviations: bt, basal tuber; btp, basipterygoid process; cer, cerebral hemisphere; de, dorsal expansion; floc, floccular process; ic, cerebral branch of the internal carotid artery; lvs, lateral venous sinus; oc, occipital condyle; ocv, orbitocerebral vein; ot, olfactory tract; pit, pituitary; sp., sphenoid artery; I–XII, cranial nerves. Scale = 25 mm.

teresae, although there are no illustrations of the external exit of these structures. In MPC–D 100/1353, there is a shallow recess ventral to the paroccipital process, in which there is a small oval opening. It is not possible to observe in the CT scans the columellar passage (though which runs the columella to reach the fenestra ovalis) and the location of the fenestra ovalis remains doubtful (Fig. 6F).

Cranial nerves V and VII both open separately within the same large and irregular teardrop-shaped recess, bounded probably by the prootic posteriorly and the laterosphenoid anteriorly (Fig. 6C,F). Within the recess, the ventral and larger foramen corresponds to CN V, whereas the smaller posterior foramen is CN VII.

There are only two small foramina for CNs II–VI, located anterodorsal to CN V and facing anteriorly reason why they are not observed in lateral view (Fig. 6C,F). The most anterior foramen corresponds to CN II, whereas the posterior one corresponds probably to CNs III and IV. The orbitocerebral vein was identified in the CT scans, but the external foramen on the braincase is difficult to observe. Based on the orientation of the proximal section of the passage, its position is dorsal to CN II (Fig. 7).

Basal tubera and basipterygoid processes are robust and short protuberances projected ventrally from the basicranium. The basicranial box, delimited between basipterygoid processes anteriorly and basal tubera posteriorly, is transversely wider than its anteroposterior length (Fig. 6A). The cerebral branch of the internal carotid artery enters the basicranium through a large slit-like foramen (15 mm maximum diameter) located dorsal to the basipterygoid process (Fig. 6B,E). In lateral view of the braincase, the crista prootica is a low vertical ridge dorsal to the basipterygoid process. It extends from the posterodorsal margin of cranial nerve (CN) V (trigeminal) to the posterodorsal corner of the internal carotid artery foramen (Fig. 6B). The small foramen anteroventral to CN V leads into the pituitary fossa and probably corresponds to the sphenoid artery (Baumel and Witmer, 1993). The ventral area of the basisphenoid between the basal tubera and the basipterygoid processes bears deep grooves and furrows left probably by blood vessels, as in *T. plicatospineus*.

As in other ankylosaurs, the ethmoidal elements (sphenethmoids and mesethmoid, Ali et al., 2008) in *T. teresae* are ossified. They enclose the olfactory tracts and the olfactory bulbs, which do not leave clear impressions on the ventral side of the frontals. The passage for the olfactory tract (indicated as CN I in the figures) is large and oval, delimited by the ossified ethmoidal elements lateroventrally and by the frontals dorsally (Fig. 6C,F). In *T. teresae*, the ethmoidal elements are anteroposteriorly short and transversely wide. Ventral to the postorbital process of the laterosphenoid, the rod-like epipterygoid firmly contacts and is fused to the lateral surface of the laterosphenoid. The ridge formed by the laterosphenoid and the epipterygoid bar is continuous ventrally with the crista prootica. In *T. teresae*, this ridge separates the foramen for CN V posteriorly and the foramina for CNs II and III anteriorly (Fig. 6C).

3.2.2. Cranial endocast

The general morphology of the cranial endocast of *T. teresae* is more similar to that of *Euoplocephalus* (Miyashita et al., 2011) than *Talarurus*, being tall and robust. The forebrain, midbrain, and hindbrain form a gentle sigmoidal shape in lateral view (Fig. 7B). The dorsal longitudinal sinus is developed enough to obscure the dorsal morphology of the brain. However, it does not form a marked dorsal expansion. In turn, the lateral venous sinus developed dorsal to the passage of the metotic foramen form large prominences.

The visible structures of the forebrain in the endocast correspond to the olfactory bulbs and olfactory tracts, cerebral hemispheres, pituitary and CN II. The olfactory tract is remarkably short. The olfactory bulbs are not reconstructed in the digital cranial endocast because they did not leave distinct impressions on the ventral sides of the frontals (Fig. 7C). The widest transverse section of the endocast corresponds to the cerebral hemispheres, which are neither particularly large nor well developed laterally (Fig. 7C). Lateroventral to each cerebral hemisphere, there is a small and long vascular passage for the orbitocerebral vein, as observed in the ankylosaurids *Euoplocephalus* (Miyashita et al., 2011) and *Talarurus* (Figs. 5C, 7). As mentioned, the exit foramen for this blood vessel is not observed in the digital braincase, but is probably positioned high on the laterosphenoid near to the contact with the frontal (Fig. 7). The pituitary is large and projects from the ventral surface of the endocast. The infundibular stalk is transversely wide and

projects slightly anteroventrally. The pituitary is slightly compressed anteroposteriorly. The distal end of the pituitary is continuous laterally with the large passages for the internal carotid arteries. Both the pituitary and the carotid arteries form a straight, bar-shaped structure because the passages form an angle of 180° between each other. The root of CN II is located anterodorsal to the infundibular stalk. The passage for this nerve is short and extends laterally and slightly ventrally.

The visible mesencephalic (midbrain) structures in the cranial endocast consist of CNs III and IV. There is a single passage anterodorsal to CN V (Fig. 7B). It probably corresponds to both CNs III and IV, as in *Euoplocephalus* (Miyashita et al., 2011, their fig. 7A).

The visible features of the hindbrain region of the endocast include the region occupied by the cerebellum, the medulla oblongata and CNs V–XII. The dorsal expansion corresponds to the cast of the sagittal longitudinal venous sinus developed dorsal to the hindbrain and midbrain and is not well expanded dorsally (Fig. 7). The floccular process of the cerebellum is a well-defined pyramidal projection on the lateral side of the endocast, posterodorsal to the roots of CNs V–VII and clearly associated to the transverse venous sinus developed dorsal to the trigeminal nerve. The large root of CN V is positioned posterodorsal to the base of the infundibulum. The passage for this nerve projects lateroventrally to exit the braincase through a large foramen posterodorsal to the internal carotid foramen. The passage for CN VII has a smaller diameter and extends dorsal and very close to the passage of CN V. Both nerves exit the braincase through separate foramina, although both openings are within a single recess. Only the roots of CN VI were reconstructed because the small passages are not seen in the CT scans. In *Talarurus*, this nerve exits the braincase through a small foramen anteroventral to CN V, which would have been the case in *T. teresae* as well. Cranial nerve VIII is not observed in the CT scans. The roots of CNs IX–XI merge into a single passage that extends laterally to exit the braincase through the metotic foramen (Fig. 7). In turn, the metotic foramen opens within a larger recess together with the foramen of the anterior branch of CN XII (Fig. 7B). The large root of the metotic passage merges dorsally with a vertical ridge on the lateral side of the endocast that represents a well-developed lateral vascular venous sinus. Cranial Nerve XII has three separate branches – two posterior ones (the most posterior one is only reconstructed at its base on the right side) and one anterior one that leaves the endocranial cavity through a foramen that merges distally with the metotic foramen (Figs. 6G, 7B). The posterior branches exit the braincase through a single external foramen lateral to the occipital condyle.

3.2.3. Inner ear

The inner ear of *T. teresae* is only partially visible in the CT scans. The visible sections correspond mainly to the distal region of the lagena and fragments of the three semicircular canals (Fig. 8). The three semicircular canals are robust, and the preserved regions suggest that they were approximately oval. The angle formed between the anterior and posterior semicircular canals is approximately 90° in dorsal view (Fig. 8B). The lagena is cylindrical and markedly long, with a slightly broaden distal end. When compared with those of most dinosaurs the lagena in *T. teresae* is markedly long, as also described for *Euoplocephalus* (Miyashita et al., 2011).

4. Ankylosaurid braincase and neuroanatomy

4.1. General braincase morphology

Braincase characters in general are not used in dinosaur phylogenies, although preliminary work showed that this set of characters is not as conservative as initially thought (Rauhut, 2007; Paulina-Carabajal, 2009). In this sense, endocranial characters are used or tested even less. Although the sample of ankylosaur taxa studied is still too poor to be analyzed statistically, the new information on ankylosaurid braincases adds anatomical data, with potential use in determining the taxonomy and phylogeny of the group. The braincase and endocranial variability between ankylosaurids and nodosaurids is poorly understood, which is also true among ankylosaurids (Figs. 9, 10).

All ankylosaurs have robust and low braincases and low and massive basicrania. There is a complete lack of pneumatic cavities such as subcondylar recess, basisphenoid recess and subsellar recess. Overall, the ankylosaur basicrania are even more conservative than in most dinosaurs, showing highly low variability except for few examples (e.g. in most ankylosaurs the exoccipital participates on the occipital condyle, whereas in others (e.g., *Sauropelta*, YPM 5529) the condyle is formed only by the basioccipital). Interestingly, ankylosaurs have ossified ethmoidal elements, which remain unossified in most saurischian dinosaurs (Vickaryous et al., 2004; Ali et al., 2008; Paulina-Carabajal and Currie, 2012), although they are commonly found in different groups of ornithischians (identified as “presphenoid”; ‘sphenethmoid’ = “accessory ossification” in Maryańska, 1977), including hadrosaurs (e.g., Horner, 1992; Evans et al., 2009), stegosaurs (Galton, 1988), and ceratopsians (Forster, 1996). The lack of sutures however, prevents further comparisons within the clade.

The number and relative positions of cranial foramina are also variable, except for few nervovascular foramina which size and position are characteristic of most ankylosaur taxa (e.g., the internal carotid artery foramen is markedly large and opens on the lateral side of the basisphenoid); internally the internal carotid passage extends transversely to enter the pituitary fossa laterally rather than posteroventrally - which is the situation observed in most dinosaurs-, all the branches of the trigeminal nerve leave the endocranial cavity through a single, large foramen (except in *Saichania*, see below). There is a tendency to the reduction of the number of foramina for those cranial nerves that exit the braincase anterior to the trigeminal nerve (CN V), and for CNs IX–XII (see discussion about this issue in Averianov, 2002) (Fig. 9). This is probably related to a particular arrangement of the muscular

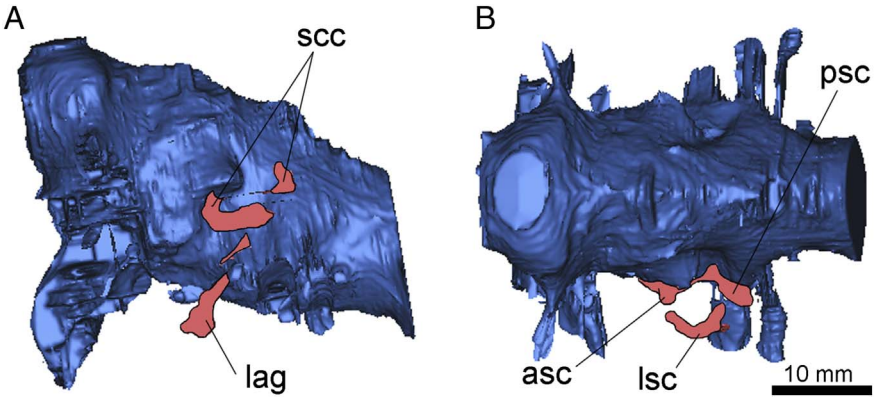

Fig. 8. Cranial endocast and partial digital reconstruction of the inner ear of *Tarchia teresae* (MPC-D 100/1353) in left lateral (A) and dorsal (B) views. The brain is also included in the figure to facilitate the interpretation of the incomplete structures. Abbreviations: asc, anterior semicircular canal; lag, lagena; lsc, lateral semicircular canal; psc, posterior semicircular canal; scc, semicircular canals. Scale bar = 10 mm.

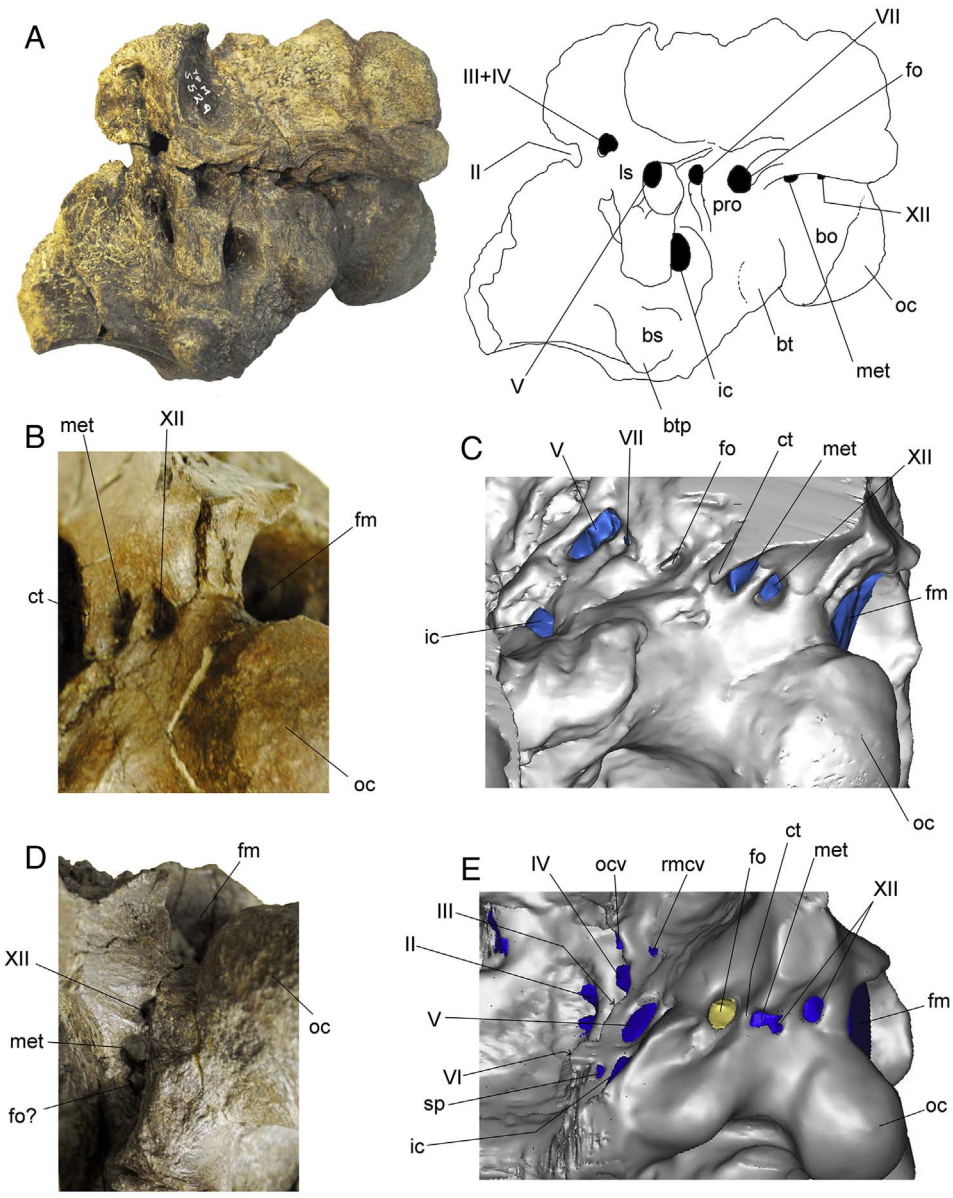

Fig. 9. North American nodosaurid braincases in left lateral view, detailed regions with cranial neurovascular foramina. A) *Sauropelta edwarsi*, YPM 5529, photograph (left) and line drawing (right); B,C) *Panoplosaurus* (= *Edmontonia*), ROM 1215, photograph of posterior cranial foramina and digital reconstruction of the braincase showing neurovascular foramina; D), *Paleoscincus rugodensis*, USNM V011868, photograph of posterior cranial foramina; E), *Pawpawsaurus campbelli*, FWMSH93B.00026, digital reconstruction of the braincase (image flipped horizontally). Abbreviations: bo, basioccipital; bs, basisphenoid; bt, basal tuber; btp, basipterygoid process; ct, crista tuberalis (probably a real crista interfenestralis); fm, foramen magnum; fo, fenestra ovalis; ic, foramen for the cerebral branch of the internal carotid artery; ls, laterosphenoid; met, metotic foramen (for CNs IX–XI); oc, occipital condyle; pro, prootic. Not to scale.

attachments and pneumaticity surrounding the braincase, and the pathways of the nerves and blood vessels once they exit the braincase that remain restricted to certain areas. The number of posterior external foramina (CNs IX–XII) in the Mongolian species is variable – there are two external foramina for CNs IX–XII in *T. teresae* and *Pinacosaurus* (Maryańska, 1977), three external foramina in *Talarurus* (four, in Marianska 1977), and only a single foramen in *Saichania* (Maryańska, 1977; Tumanova, 1987; Averianov, 2002). Regarding CN XII, there are three separate branches emerging from three external foramina in the ankylosaurid *Bissektipelta* (Averianov, 2002), and there are two foramina in *Sauropelta* (YPM 5529); whereas most nodosaurids have a single foramen for the branches (e.g., *Edmontonia*, ROM 1215, USNM v 011868; *Hungarosaurus*, Ősi et al. (2014); and *Pawpawsaurus*, FWMSH93B.00026). Three separate branches for CN XII, from which the two posterior ones merge to exit through a single foramen, whereas the anterior passage merges distally with the metotic passage, are present *Euoplocephalus* (Miyashita et al., 2011), *Talarurus* and *T. teresae* (a possible branch is observed in the left side of the cranial endocast of *Pawpawsaurus*, Paulina-Carabajal et al., 2016a). Because the number of external openings on the braincase does not necessarily reflect the number of passages used by the cranial nerves to leave the endocranial cavity, the number of external cranial nerve openings should be used carefully as a state of character.

4.2. Cranial endocast morphologies among ankylosaurs and neurosensorial capabilities

Endocranial morphology is conservative in the ankylosaur taxa studied, which are characterized by a short forebrain with markedly short olfactory tracts and small olfactory bulbs, poorly marked cephalic and pontine flexures, and a large pituitary that projects mostly ventrally (except in *Kumbarrasaurus*, which has a relatively smaller and posteroventrally oriented pituitary, more similar to the condition observed in most dinosaurs) (Fig. 10). The nodosaurid cranial endocast is relatively more sigmoidal in lateral view than that of an ankylosaurid, this probably related to the head-neck position. In turn, the ventral side of the medulla oblongata is mostly flat in ankylosaurids (Fig. 10A–C), but convex in most nodosaurids (is flat in *Struthiosaurus* YPM 57173), this probably related to the presence of larger ventral longitudinal venous sinuses (Witmer et al., 2008) in the latter group (Fig. 10E–I). Also, larger dorsal expansions or dural peaks –a structure that responds to the degree of development of the dorsal longitudinal sinus– are observed in

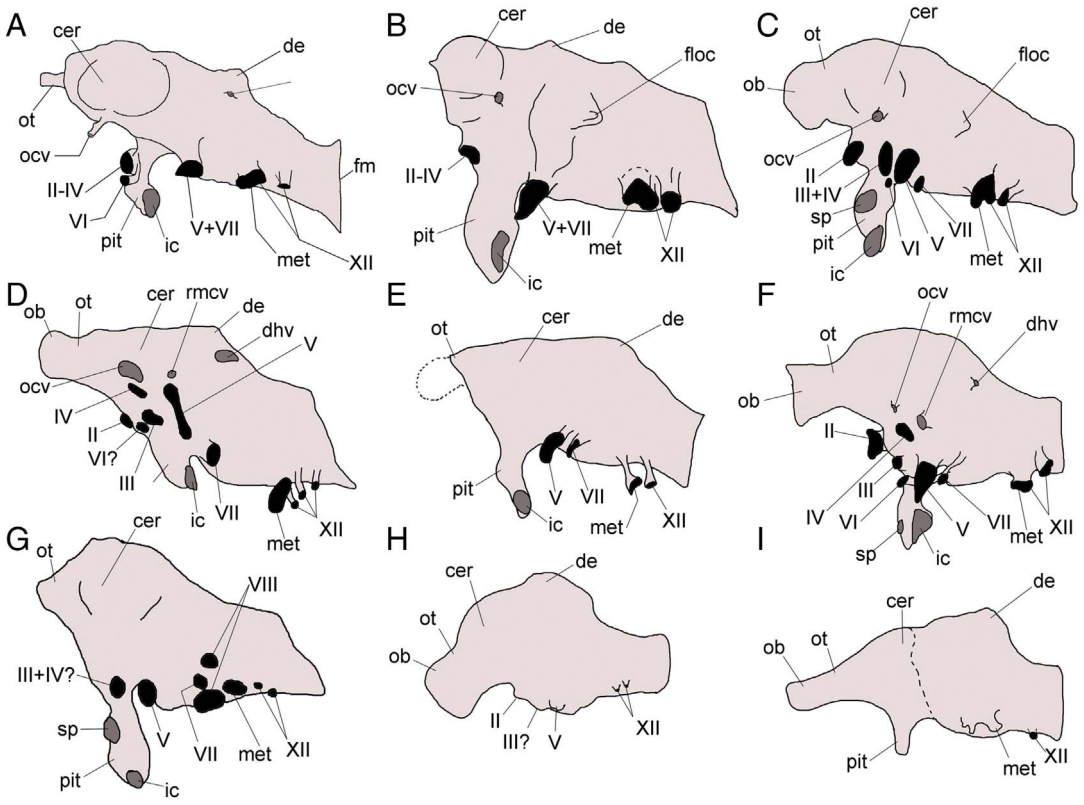

Fig. 10. Ankylosaur cranial endocasts in left lateral view. A) *Talarurus*; B) *T. teresae*; C) *Euoplocephalus*; D) *Kunbarrasaurus*; E) *Panoplosaurus*; F) *Pawpawsaurus* (flipped horizontally); G) cf. *Polacanthus*; H) *Struthiosaurus transilvanicus* and I) *Hungarosaurus*. Abbreviations: cer, cerebral hemisphere; de, dorsal expansion; dhv, dorsal head vein; fm, foramen magnum; ic, cerebral branch of the internal carotid artery; met, metotic passage (for CNs IX–XI); ob, olfactory bulb; ocv, orbitocerebral vein; ot, olfactory tract; pit, pituitary; rmcv, rostral middle cerebral vein; sp., sphenoid artery; II–XII, cranial nerves. (C,D, redrawn from Leahey et al., 2015; F, redrawn from Paulina-Carabajal et al., 2016a; G–I, redrawn from Ősi et al., 2014). Not to scale.

nodosaurids (Fig. 10E–I). In comparison, the basal ankylosaur *Kunbarrasaurus* (Leahey et al., 2015, their fig. 10A) and ankylosaurids have relatively smaller dorsal expansions (Fig. 10A–C). Ősi et al. (2014) discuss the implications of a well-developed "cerebellum" in European nodosaurids and the implications for locomotion. However, the enlarged cerebella described for *Hungarosaurus* and *Struthiosaurus* correspond more likely to an enlargement of the endocranial cavity due the presence of an expanded dorsal longitudinal venous sinus.

The presence of the flocculus of the cerebellum seems to be characteristic of ankylosaurids, and has not been described in any known nodosaurid cranial endocast so far. The floccular process was previously identified in the cranial endocast of *Euoplocephalus* (Miyashita et al., 2011) and the floccular recess (its osteological correlate) in the endocranial cavity of *Talarurus* (Maryańska, 1977), and now in *T. teresae*. In each of these cases, the soft structure was large enough to leave an impression on the anterior wall of the vestibular eminence. These structures are relatively large for non-theropod dinosaurs such as sauropods. However, the paleobiological implications of the development of the flocculus in quadrupedal extinct reptiles remain unknown. Within saurischian dinosaurs, floccular processes are present in theropod cranial endocasts and in few non-titanosaurid sauropodomorphs (Janensch, 1935–1936; Sereno et al., 2007; Knoll and Schwarz-Wings, 2009; Paulina-Carabajal et al., 2016b). Because the flocculus is larger in flying reptiles it was initially correlated with more complex coordination needed during the flight (Witmer et al., 2003). More recent studies indicated that the sizes and function of the flocculus are related to capabilities for gaze stabilization (Walsh et al., 2013). Because of this, the presence of floccular process in ankylosaurids was interpreted as a greater capability for active head movements than nodosaurids because the swinging actions of heavy tail clubs may require greater control to balance the body (Paulina-Carabajal et al., 2016a). Although a more recent work based on extant mammals and birds indicates that the size of the floccular recess is not a reliable proxy of behavior in vertebrates (Ferreira-Cardozo et al., 2017), the presence of the floccular recess in the three ankylosaurids and its absence in the six nodosaurids (see Miyashita et al., 2011; Ősi et al., 2014; Paulina-Carabajal et al., 2016a) suggest that may be a useful anatomical trait to differentiate –if not the paleoneurologies or the paleobiologies – the endocranial morphologies of the two families of ankylosaurs.

The complete morphology of the inner ear is only known for a few number of ankylosaur species (*Euoplocephalus*, *Kunbarrasaurus*, *Pawpawsaurus*, and partially in *Tarchia*), and all taxa seem to have robust and low semicircular canals. The length of the lagena, however, is variable between the groups, being markedly elongate in *Euoplocephalus*, *Tarchia teresae*, and probably *Talarurus*, suggesting that this is a particular characteristic for the family. The nodosaurid inner ear morphology is poorly known, and *Pawpawsaurus* is the only taxon in which it has been completely reconstructed and described so far (Paulina-Carabajal et al., 2016a), being conical and short, as in most dinosaurs. The basal ankylosaur *Kunbarrasaurus* has probably also a short lagena (Leahey et al., 2015, their fig. 10). There are no dinosaurs with such long lagena as observed in the mentioned ankylosaurids, suggesting that hearing (mostly in the lower range of frequencies) was an important sense for this group (Miyashita et al., 2011). Although based on an extremely small sample of braincases, this suggests that ankylosaurids may have had a wider range of sound perception within the clade. Because animals are adapted to produce sounds that can be heard by their own species (e.g., Witmer and Ridgely, 2008; Miyashita et al., 2011), the different sizes of the lagena within ankylosaurs may respond to different capabilities of sound production and sound perception within the two families.

5. Conclusions

During the past decade, the use of CT scans has revealed not only the details of internal traits – such as the brain and paleoneurology of certain groups of dinosaurs – but also allowed the virtual extraction of braincases from articulated skulls, providing significant anatomical information. The general morphology of the ankylosaur braincase is conservative within the group. The braincase is robust and low with ossified ethmoidal elements and an apneumatic basicranium. The Asian ankylosaurids exhibit variation in the following characters: shape of the paroccipital process, shape of foramen magnum, shape and orientation of the occipital condyle, presence/absence of keeled ventral margin on the condyle, presence of transverse grooves lateral to the foramen magnum and below the exoccipital protuberance, and the number of cranial nervovascular foramina. This number of foramina is variable, except for the presence of a large opening for the cerebral internal carotid artery and a large single trigeminal foramen. There is a tendency for the reduction of the number of anterior cranial foramina (CNs II–IV may exit the braincase through a single foramen), as well as the posterior ones (e.g., three, two or one foramen for CN XII).

The endocranial morphology is conservative but shows some degree of variation between Ankylosauridae and Nodosauridae. The endocranial casts of Ankylosauridae and Nodosauridae show some differences including the angles between the forebrain, midbrain, and hindbrain, which tend to be less marked in ankylosaurids than in nodosaurids. The dorsal longitudinal venous sinuses, is relatively greater in nodosaurids than in ankylosaurids. The presence of the flocculus and an elongate lagena in ankylosaurid taxa suggest that this group may have had better development of gaze stabilization and the ability to hear a greater range of sound frequencies respectively. However, there are no isolated endocranial traits that can be used to distinguish between species so far.

Acknowledgments

Thanks go to all members of the Korea-Mongolia International Dinosaur Project (KID) that participated during the 2007 and 2008 fieldwork. The authors thank Dr. Jae-Hwa Jin (KIGAM) for allowing the use of the Industrial CT scanner under his care. We thank the collection managers D. Brinkman (YPM), M. Carrano (NMNH) and D. Evans (ROM), for the access to the specimens under their care. We are thankful to the Editor in Chief Prof. T. Algeo and to the Special Issue Editor F. Fanti, V. Arbour (ROM) and an anonymous reviewer for their comments and corrections, which greatly improved this manuscript. The KID expedition was supported by a grant from Hwaseong City, Gyeonggi Province, South Korea (to YNL). This work was also supported by the Basic Research in Application and Development of Geological Samples and Geo-technology R&D Policy [grant number 17-3117-2 to HJL], the National Research Foundation of Korea [grant number 2016R1A2B2015012 to YNL], and Agencia Nacional de Promocion Cientifia y Tecnologica [grant number PICT 2012/1425 and PICT 2016-0481 to APC].

References

Ali, F., Zelenitsky, D.K., Therrien, F., Weishampel, D.B., 2008. Homology of the 'ethmoidal complex' of tyrannosaurids and its implications for the reconstruction of the olfactory apparatus of non-avian theropods. J. Vertebr. Paleontol. 28, 123–133.

Arbour, V.M., Currie, P.J., 2016. Systematics, phylogeny and palaeobiogeography of the ankylosaurid dinosaurs. J. Syst. Palaeontol. http://dx.doi.org/10.1080/14772019.2015.1059985.

Arbour, V.M., Currie, P.J., Badamgarav, D., 2014. The ankylosaurid dinosaurs of the Upper Cretaceous Baruungoyot and Nemegt formations of Mongolia. Zool. J. Linnean Soc. 172, 631–652. http://dx.doi.org/10.1111/zoj.12185.

Averianov, A., 2002. An ankylosaurid (Ornitischia: Ankylosauria) braincase from the Upper Cretaceous Bissekty formation of Uzbekistan. Bull. Inst. R. Sci. Nat. Belg. 72, 97–110.

Baumel, J., Witmer, L.M., 1993. Osteology. In: Baumel, J., King, A.S., Breazile, J.E., Evans, H.E., Vanden, J.C. (Eds.), Handbook of Avian Anatomy: Nomina Anatomica Avium. Publications of the Nuttall Ornithological Club, Cornell, pp. 45–132.

Carpenter, K., Kirkland, J.I., Burge, D., Bird, J., 2001. Disarticulated skull of a new primitive ankylosaurid from the Lower Cretaceous of eastern Utah. In: Carpenter, K. (Ed.), The Armored Dinosaurs. Indiana University Press, Bloomington, pp. 211–238.

Coombs, W.P., 1978. An endocranial cast of *Euoplocephalus* (Reptilia, Ornithischia). Palaeontogr. Abt. A 161, 176–182.

Currie, P.J., 1997. Braincase anatomy. In: Currie, P.J., Padian, K. (Eds.), Encyclopedia of Dinosaurs. Academic Press, pp. 81–83.

Eberth, D.A., 2017Eberth, in press. Stratigraphy and paleoenvironmental evolution of the dinosaur-rich Baruungoyot-Nemegt succession (Upper Cretaceous), Nemegt Basin, southern Mongolia. Palaeogeogr. Palaeoclimatol. Palaeoecol. http://dx.doi.org/10.1016/j.palaeo.2017.11.030. (in press).

Evans, D.C., 2006. New evidence on brain-endocranial cavity relationships in ornithischian dinosaurs. Acta Palaeontol. Pol. 50, 617–622.

Evans, D., Ridgely, R., Witmer, L.M., 2009. Endocranial anatomy of Lambeosaurine hadrosaurids (Dinosauria: Ornithischia): a sensorineural perspective on cranial crest function. Anat. Rec. 292, 1315–1337.

Ferreira-Cardozo, S., Aráujo, R., Martins, N.E., Walsh, S., Martins, R.M.S., Kardjilov, N., Manke, I., Hilger, A., Castanhinha, R., 2017. Floccular fossa size not a reliable proxy of ecology and behavior in vertebrates. Sci. Rep. 7. http://dx.doi.org/10.1038/s41598-017-01981-0.

Forster, C.A., 1996. New information on the skull of triceratops. J. Vertebr. Paleontol. 16, 246–258.

Galton, P.M., 1983. Armored dinosaurs (Omithischia: Ankylosauria) from the Middle and Upper Jurassic of Europe. Palaeontogr. Abt. A 182, 1–25.

Galton, P.M., 1988. Skull bones and endocranial casts of stegosaurian dinosaur Kentrosaurus Hennig, 1915 from Upper Jurassic of Tanzania, East Africa. Geol. Palaeontol. 22, 123–143.

Gilmore, C.W., 1933. On the dinosaurian fauna of the Iren Dabasu Formation. Bull. Am. Mus. Nat. Hist. 67, 23–78.

Hawakaya, H., Manabe, M., Carpenter, K., 2005. Nodosaurid ankylosaur from the Cenomanian of Japan. J. Vertebr. Paleontol. 25, 240–245.

Horner, J.H., 1992. Cranial morphology of *Prosaurolophus* (Ornitischia: Hadrosauridae) with descriptions of two new hadrosaurid species and an evaluation of hadrosaurid phylogenetic relationships. Museum of the rockies. Occas. Pap. 2, 1–80.

Janensch, W., 1935–1936. Die Schadel der Sauropoden *Brachiosaurus*, *Barosaurus* und *Dicraeosaurus* aus der Tendaguru-Schichten Deutsch-Ostafrikas. Palaeontography (Suppl. 7), 147–298.

Knoll, F., Schwarz-Wings, D., 2009. Paleoneuroanatomy of *Brachiosaurus*. Ann. Paleontol. 95, 165–175.

Kurzanov, S.M., Tumanova, T.A., 1978. Endo-cranium structure of some Mongolian ankylosaurs. Paleontol. Zh. 3, 90–96.

Leahey, L.G., Molnar, R.E., Carpenter, K., Witmer, L.M., Salisbury, S., 2015. Cranial osteology of the ankylosaurian dinosaur formerly known as *Minmi* sp. (Ornithischia: Thyreophora) from the Lower Cretaceous Allaru mudstone of Richmond, Queensland, Australia. PeerJ 3, e1475. http://dx.doi.org/10.7717/peerj.1475.

Lee, Y.-N., 1996. A new nodosaurid ankylosaur (Dinosauria: Ornitischia) from the Paw Paw formation (Late Albian) of Texas. J. Vertebr. Paleontol. 16, 232–245.

Maleev, E.A., 1952. A new ankylosaur from the Upper Cretaceous of Asia. Dokl. Akad. Nauk Soiuza Sov. Sotsialisticheskikh Resp. 87, 273–276 (in Russian).

Maryańska, T., 1977. Ankylosauridae (Dinosauria) of Asia. Palaeontol. Pol. 37, 85–151.

Miyashita, T., Arbour, V., Witmer, L., Currie, P., 2011. The internal cranial morphology of an armoured dinosaur Euoplocephalus corroborated by X-ray computed tomographic reconstruction. J. Anat. 219, 661–675.

Norman, D.B., Faiers, T., 1996. On the first partial skull of an ankylosaurian dinosaur from the Lower Cretaceous of the Isle of Wight, southern England. Geol. Mag. 133, 299–310.

Ősi, A., Pereda Suberbiola, X., Földes, T., 2014. Partial skull and endocranial cast of the ankylosaurian dinosaur *Hungarosaurus* from the Late Cretaceous of Hungary: implications for locomotion. Palaeontol. Electron. Vol. 17 (Issue 1; 1A). palaeo-electronica.org/content/2014/612-skull-of-hungarosaurus (18 p.).

Parish, J.C., Barrett, P.M., 2004. A reappraisal of the ornithischian dinosaur Amtosaurus magnus Kurzanov and Tumanova 1978, with comments on the status of A. archibaldi Averianov 2002. Can. J. Earth Sci. 41, 299–306.

Paulina-Carabajal, A., 2009. The braincases of Argentinean theropod dinosaurs: osteology and phylogenetic implications. J. Vertebr. Paleontol. 30 (Abstracts: 162A).

Paulina-Carabajal, A., Currie, P.J., 2012. New information on the braincase and endocast of *Sinraptor dongi* (Theropoda: Allosauroidea): ethmoidal region, endocranial anatomy and pneumaticity. Vertebrata PalAsiatica 50, 85–101.

Paulina-Carabajal, A., Lee, Y.-N., Jacobs, L.L., 2016a. Neuroanatomy of the primitive nodosaurid dinosaur *Pawpawsaurus campbelli* and paleobiological implications of some endocranial features. PLos One 11 (3), e0150845. http://dx.doi.org/10.1371/journal.pone.0150845.

Paulina-Carabajal, A., Canale, J.I., Haluza, A., 2016b. New rebbachisaurid cranial remains (Sauropoda, Diplodocoidea) from the Cretaceous of Patagonia, Argentina, and the first endocranial description for a South American representative of the clade. J. Vertebr. Paleontol. http://dx.doi.org/10.1080/02724634.2016.1167067.

Penkalski, P., Tumanova, T., 2017. The cranial morphology and taxonomic status of *Tarchia* (Dinosauria: Ankylosauridae) from the Upper Cretaceous of Mongolia. Cretac. Res. 70, 117–127.

Pereda Suberbiola, J., Galton, P.M., 1994. Revision of the cranial features of the dinosaur *Struthiosaurus austriacus* Bunzel (Ornithischia: Ankylosauria) from the Late Cretaceous of Europe. N. Jb. Geol. Paläont. (Abh.) 191, 173–200.

Porter, W.R., Sedlmayr, J.C., Witmer, L.M., 2016. Vascular patterns in the heads of crocodilians: blood vessels and sites of thermal exchange. J. Anat. http://dx.doi.org/10.1111/joa.12539.

Rauhut, O.W.M., 2007. The myth of the conservative character: braincase characters in theropod phylogenies. Hallesches Jahrb. Geowis 23, 51–54.

Sereno, P.C., Wilson, J.A., Witmer, L.M., Whitlock, J.A., Maga, A., et al., 2007. Structural extremes in a Cretaceous dinosaur. PLoS One 2 (11), e1230. http://dx.doi.org/10.1371/journal.pone.0001230.

Thompson, R.S., Parish, J.C., Maidment, S.C.R., Barrett, P.M., 2012. Phylogeny of the ankylosaurian dinosaurs (Ornithischia: Thyreophora). J. Syst. Palaeontol. 10, 301–312. http://dx.doi.org/10.1080/14772019.2011.569091.

Tumanova, T.A., 1987. The armored dinosaurs of Mongolia. Transactions of the joint Soviet-Mongolian Paleontological. Expedition 32, 1–76.

Vickaryous, M.A., Russell, A.P., 2003. A redescription of the cranium of *Euoplocephalus tutus* (Archosauria: Ornithischia): a foundation for comparative and systematic studies of ankylosaurian dinosaurs. Zool. J. Linnean Soc. 137, 157–186. http://dx.doi.org/10.1046/j.1096-3642.2003.00045.x.

Vickaryous, M.A., Maryánska, T., Weishampel, D.B., 2004. Ankylosauria. In: Weishampel, D.B., Dodson, P., Osmólska, H. (Eds.), The Dinosauria. University of California Press, Berkeley, pp. 363–392.

Walsh, S.A., Iwaniuk, A.N., Knoll, M.A., Bourdon, E., Barrett, P.M., Milner, A.C., Nudds, R.L., Abel, R.L., Dello Sterpaio, P., 2013. Avian cerebellar floccular fossa size is not a proxy for flying ability in birds. PLoS ONE 8 (6), e67176. http://dx.doi.org/10.1371/journal.pone.0067176.

Witmer, L.M., Ridgely, R.C., 2008. The paranasal air sinuses of predatory and armored dinosaurs (Archosauria: Theropoda and Ankylosauria) and their contribution to cephalic structure. Anat. Rec. 291, 1362–1388.

Witmer, L.M., Chatterjee, S., Franzosa, J., et al., 2003. Neuroanatomy of flying reptiles and implications for flight, posture and behavior. Nature 425, 950–953.

Witmer, L.M., Ridgely, R.C., Dufeau, D.L., et al., 2008. Using CT to peer into the past: 3D visualization of the brain and ear regions of birds, crocodiles, and nonavian dinosaurs. In: Endo, H., Frey, R. (Eds.), Anatomical Imaging: Towards a New Morphology. Springer, Tokyo, pp. 67–87.